SPE 107391

Streamline-Based Simulator for Unstructured Grids

M. Pomata and A. Menéndez, Consultants, and J. Valle, SPE, Interfaces

This paper was prepared for presentation at the 2007 SPE Latin American and Caribbean Petroleum Engineering Conference held in Buenos Aires, Argentina, 15–18 April 2007.

Abstract

Oil recovery operations are strongly conditioned by a series of complex phenomena that take place in the reservoir. Presently, it is common to use numerical modeling tools for the oilfield development.

In this paper we present the first implementation step of a streamline-based simulator for unstructured grids. In this stage, we focus on a 2D incompressible flow model. Streamline flow simulation has been extensively used for the past ten years, and it is now used as an effective and complementary tool to more traditional flow modeling approaches, such as finite differences.

Streamline-based simulation is suitable for large, geologically complex and heterogeneous systems, where fluid flow is dictated by well rates, rock properties, fluid mobility and gravity. Capillary effects and expansion-dominated systems are not modeled correctly using streamlines.

The mathematical model is based on the mass conservation of the three-phase system.

The basic hypothesis, as well as the mathematical model on which the streamline-based simulator stand, are presented in some detail.

We use the finite volume scheme as the numerical method for the discretization of the differential equations. Trinodal triangular elements are used. The pressure equation formulation is space centered with an upstream formulation for the phases mobilities and is solved using a direct skyline solver[2]. The 1D saturation equation is discretized using an explicit finite difference scheme in time and an upstream formulation in space.

The results obtained by our streamline-based simulator are compared with known analytical solutions (such as Buckley-Leverett flow) and with our previous full implicit black oil simulator. Good quantitative agreement is obtained.

Introduction

Numerical reservoir simulation is a widely used tool for production enhancement, reservoir characterization and understanding of fluid flow performance. The more realistic the physical and reservoir models are, the more accurate is the answer obtained.

Many techniques have been developed to obtain more realistic geological models, such as geostatistical models, and laboratory techniques.

Therefore, as the complexity of reservoir modeling has been increasing, the difficulties in solving them have increased as well. Nowadays, it is not strange to find reservoir models on the order of 10^6 gridblocks. One solution to this problem is the improvement of the hardware used to solve them, such as cluster parallelization and the processors speed. The other approach is the improvement of simulation methods themselves. This is the case of streamline simulation.

Streamline-based simulation relies on the fact that there are, at least, two distinct time scales in the process of field scale fluid flow through porous media. The time scale of pressure diffusion is much smaller than the time scale of saturation diffusion, so the quasi-stationarity hypothesis can be used. This decouples the pressure and saturation dynamic problems. Then, changing variables to the "time of flight" i.e., a parameter along streamlines, the full 2D/3D problem converts into multiple 1D problems solved along streamlines. The underlying idea is to merge the Lagrange and Euler flow approaches.

Once the pressure field is calculated, the streamline paths are univocally determined and traced from injectors to producers. Then, saturations are moved along a "natural" streamlines grid until the pressure field is recalculated and the cycle is repeated. This makes the streamlines method an IMPES numerical method.

Solving the 1D saturation equation along the streamline grid instead of solving saturations between discrete gridblocks enables the use of large convective steps, making the system evolution much faster. Furthermore, for heterogeneous systems it is claimed[1] that the pressure field is a weak function of fluid properties, making the number of pressure updates very small.

The ability to take large convective steps and only update the streamline paths periodically is the primary reason why streamline-based simulators are orders of magnitude faster than conventional simulators.

In the next section the basic equations and hypothesis leading to streamline theory will be shown and explained in some detail.

Statement of Theory and Definitions

The mass conservation equation for component i ($1 \le i \le NI$) distributed in phase j (where j = oil, gas or water) and neglecting gravity effects is given by:

$$H\frac{\partial}{\partial t}\left[\phi\sum_j C_{ij}\rho_j S_j\right] = \nabla.\left[H\sum_j C_{ij}\rho_j\frac{k_{rj}}{\mu_j}\overline{K}.\nabla p_j\right] + Hq_i \quad (1)$$

where we have defined:

t : time coordinate [sec]

x,y : spatial horizontal coordinates [m]

$\nabla = (\partial/\partial x, \partial/\partial y)$: gradient operator [1/m]

$H(x, y)$: thickness [m]

P_j : phase pressure [N/m^2]

$S_j(x, y)$: saturation of phase j [-]

$\phi(x, y)$: rock porosity [-]

$\rho_j(x, y)$: density of phase j [kg/m^3]

$\mu_j(x, y)$: viscosity of phase j [kg/(m.s)]

$k_{rj}(x, y)$: relative permeability of phase j [-]

C_{ij} : mass fraction of component i in phase j [-]

$\overleftrightarrow{K}(x, y)$: Absolute permeability tensor [m^2]

$q_i(x, y)$: Local mass injection/production per volume of component i [kg/(m^3.s)]

We have used Darcy's law as a phenomenological law.

Equation (1) simply states that the increase in mass of component i in an elemental volume, equals the mass flux of that component through the edges of the control volume, plus the local mass injection or production of the same component.

The streamlines model requires some additional hypothesis such as: there is no fluid compressibility, the capillary pressure and the solubilities are neglected, and pressure is solved for in a quasi-stationary state. In mathematical form:

$$\overline{\nabla}.\overline{u}_{tot} = 0$$

$$P_w = P_g = P_o$$

$$R_s = 0 = R_v \quad (2)$$

$$\frac{\partial}{\partial t} \approx 0$$

Using (2) in equations (1), and doing some algebra, we obtain the pressure and saturation equations:

$$\Delta P\,\overline{\nabla}.\left[H\lambda_T\,\overline{K}.\overline{\nabla}P\right] = -H\sum_i\frac{q_i}{\rho_i} \quad (3)$$

$$\phi\frac{\partial S_j}{\partial t} + \overline{u}_{tot}.\overline{\nabla}f_j = q_s f_{j,s} \quad (4)$$

where the summation in (3) is done over the phases injected, and we have defined:

ΔP : pressure normalization factor [N/m^2]

$\lambda_t = \sum_j \frac{k_{rj}}{\mu_j}$: total fluid mobility [(m.s)/Kg]

$\overline{u}_{tot}$: total velocity vector field

$f_j = \frac{k_{rj}/\mu_j}{\sum_m k_{mj}/\mu_m}$: Buckley-Leverett fractional flow

q_s : source (or sink, if negative) flow rate

Then, changing variables to the Time of Flight, which is a parameter along the streamlines defined as $\tau(s) = \int_0^s \frac{\phi(\zeta)}{|\overline{u}_{tot}|}d\zeta$, we obtain a 1D version of (4):

$$\frac{\partial S_j}{\partial t} + \frac{\partial f_j}{\partial \tau} = \frac{q_s f_{j,s}}{\phi} \quad (5)$$

Equation (3) was discretized using a finite volume scheme, which has the same versatility as a finite element scheme but with the additional advantage of intrinsic mass conservation. The discretization is performed on an arbitrary, eventually unstructured, grid. Details on the technique were presented elsewhere[2].

Once the pressure equation is solved, the streamlines are traced from injectors to producers using Pollock's interpolation algorithm[3,4,5]. This method use particle tracking ideas to define the streamline. The basic hypothesis of this analytical model is that the velocity field in each direction varies linearly and is independent of the velocities in the other directions, as shown in Figure 1.

Each streamline is given a flow rate that is calculated as the injection flow rate divided by the number of streamlines per injector. The beginning position of the streamlines in the injector's control volume edge is calculated as the middle of the streamtube carrying the same flow rate.

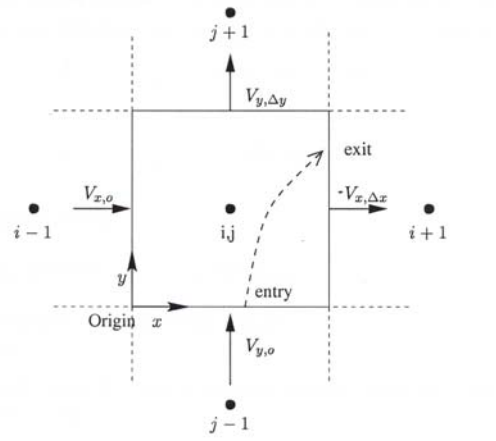

Figure 1. Pollock's interpolation geometry.

Pollock's algorithm was developed for orthogonal unit cells. As our grid is non orthogonal, an isoparametric coordinate transformation[6] was needed to transform them to an orthogonal unit cell (Figure 2). Given the four coordinates vectors $\bar{r}_0, \bar{r}_1, \bar{r}_2, and\ \bar{r}_3$ of a quadrangle's vertexes in physical space (x, y), the transformation to reference space (ζ, η) is:

$$\bar{r} = \bar{r}_0(1-\zeta)(1-\eta) + \bar{r}_1(1-\eta)\zeta + \bar{r}_2(1-\zeta)\eta + \bar{r}_3\eta\zeta \tag{6}$$

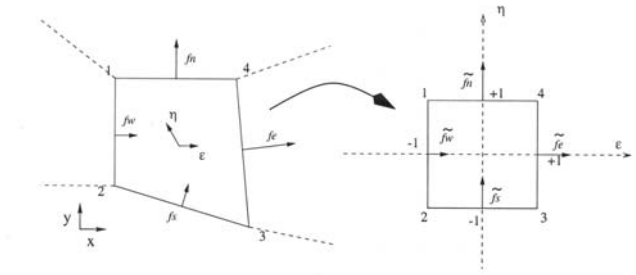

Figure 2. Geometry transformation to use Pollock's algorithm.

Furthermore, the fluxes that cross each quadrangle element boundary have to be transformed by $\tilde{f} = f / J_m \phi$ in order to ensure mass conservation, where J_m is the transformation Jacobian evaluated at the middle of the quadrangle.

Following Prèvost's tracing criteria, a sub triangular grid was introduced[4,5] in order to post-process the discontinuous velocities, leading to flux continuous velocity interpolation in the whole domain (Figure 3).

For interior grid nodes, the conditions imposed on the velocities in the new "patches" are:

$$\bar{V}_i . \hat{n}_{2,4} dl_{2,4} = f_{i,2} + f_{i,3} \tag{7}$$

$$(\bar{V}_i - \bar{V}_{i+1}) . \hat{n}_{i+} dl_{i+} = 0 \tag{8}$$

$$\sum_{i=1}^{n} \frac{\bar{V}_i . \hat{t}\, dl_i}{K_i} = 0 \tag{9}$$

where:

$\bar{V}_i$: "patch *i*" velocity

$\hat{n}_{2,4}$: outer normal to patch face 2-4

$dl_{2,4}$: length of patch segment 2-4

$f_{i,2}, f_{i,3}$: fluxes though quadrangle faces 2 and 3

$\hat{t}$: patch *i* inner edge normal

dl_{i+} : patch *i* inner edge length

For *N* convergent elements to node *i* we have 2*N* unknown velocities components. On the other hand, we have *N* conditions in (7), which simply represent mass conservation in the subtriangles. In (8) we have *N*-1 equations that impose flux conservation across the inner edges. Finally, equation (9) assures flux irrotationality. Thus, (7), (8), and (9) give the 2*N* equations necessary to solve the system.

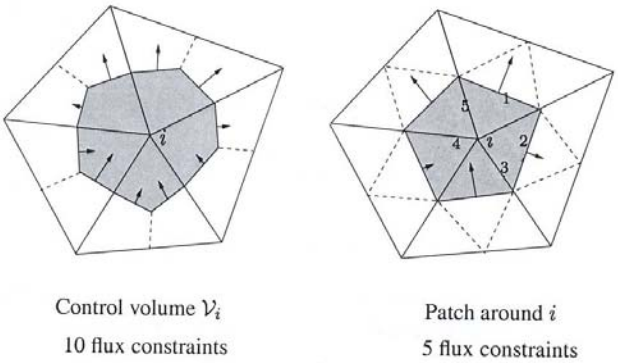

Figure 3. Prevost's post process velocities.

When the node is on the edge of the grid, condition (9) is replaced by impermeability on the edge, i.e., the patch velocity is parallel to the impermeable edge.

As an illustration, Figure 4 shows the streamlines built for the quarter of a five spot test, where fluid is injected at the lower left corner and produced at the upper right corner.

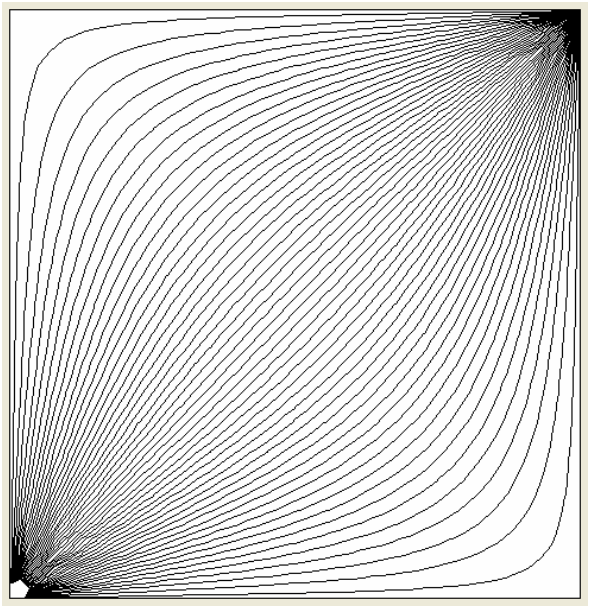

Figure 4. Example of streamlines traced from injector (lower left corner) to producer (upper right corner) using Pollock-Prèvost algorithm.

Once the streamlines are traced and the Time of Flight measured, the saturation is mapped along each streamline. The discretization of (5) was undertaken using an explicit upstream finite difference scheme. In points where no sources are present, we have:

$$S_{j,k}^{n+1} = S_{j,k}^{n} - \frac{\Delta t_{sl}^{n+1}}{\Delta \tau_{sl}} \left(f_{j,k}^{n+1} - f_{j,k}^{n} \right) \tag{10}$$

where:

j : fluid phase (oil, water, gas)
k : index that run over all the streamline nodes
n : time step index
Δt_{sl}^{n+1} : current time step for saturations evolution
$\Delta \tau_{sl}$: Time of Flight of current node

To start the saturation evolution, maximum water saturation at the injectors is imposed.
To ensure numerical stability, we limit the time-step automatically, so as information traveling with the highest advection velocity cannot proceed beyond the next streamline node (Courant condition). Then, for each streamline equation (10) is solved iteratively until the pressure-update time step Δt is reached (i.e., $\Delta t = \sum_n \Delta t_{sl}^{n}$). The pressure time step Δt_p is selected so as pressure diffusion has had enough time to proceed along the whole reservoir, i.e. $\Delta t_p \approx \phi c_r L^2 / \left(\lambda_t K \right)$, where L is the reservoir length. This time step represents the time necessary for the pressure to change significantly because of saturation (or mobility) change. Thus, between pressure changes many saturation time steps can be performed.

After saturations are updated in the streamlines grid, they must be mapped back to the underlying original grid using a Time of Flight weighting method. This is performed by averaging the properties along streamlines passing through each quadrangle, weighted with Time of Flight:

$$\left\langle S_{quad} \right\rangle = \frac{\sum_{i=1}^{N_{quad}^{SL}} \Delta \tau_i S(\tau)_i}{\sum_{i=1}^{N_{quad}^{SL}} \Delta \tau_i} \tag{11}$$

$$\left\langle \lambda_{t,quad} \right\rangle = \frac{\sum_{i=1}^{N_{quad}^{SL}} \Delta \tau_i \lambda(\tau)_i}{\sum_{i=1}^{N_{quad}^{SL}} \Delta \tau_i} \tag{12}$$

Once this is done, the process is repeated by going back to the pressure field calculation.

Presentation of Data and Results

We will present results for two problems, in order to validate the implemented numerical model. First, we will simulate the 1D immiscible two-phase displacement problem, by injecting water in a channel saturated with oil. The channel is 5000 m long (x direction), 200 m wide (y direction), and has a homogeneous depth of 10 m. The calculation grid is regular, with 100 m side triangular elements. Properties are considered as homogeneous: porosity $\Phi = 0.2$, absolute permeability $K = 10^{-13}$ m^2, rock compressibility $c_r = 5.10^{-9}$ 1/Pa, oil viscosity $\mu_o = 0.001$ Pa.s.

Water injection is applied at the three leftmost nodes from the side of the channel, two at the corners and one in the middle. The mobility ratio is equal to 1. The total injection flow rate was 6 10^{-4} m^3/s. At the producers, a constant pressure of 0.01 Pa was imposed. The relative permeability was related to saturation through the simple relation:

$$k_{ro} = k_{ot} \left(1 - S_{wd} \right)^2 \text{ and } k_{rw} = k_{wt} S_{wd}^{\ 2}$$

where $S_{wd} \equiv \left(S_w - S_{wc} \right) / \left(1 - S_{wc} - S_{or} \right)$ is the relative saturation, S_{wc} the critical water saturation, S_{or} the residual oil saturation, k_{ot} the oil relative permeability when $S_w = S_{wc,}$ and k_{wt} the water relative permeability at $S_w = 1\text{-}S_{or}$.

The numerical results are compared with Buckley-Leverett analytical solution, and with a fully implicit black oil simulator[2] (Figure 5). The agreement with the analytical solution is considered satisfactory. Deviations arise around the saturation front due to numerical diffusion. However, this effect is weaker than for the full simulator. In a second test with fluid, a mobility ratio of 10 was undertaken, with a similar degree of agreement (Figure 6). Computer time was three orders of magnitude higher for the full simulator in comparison with the streamlines simulator.

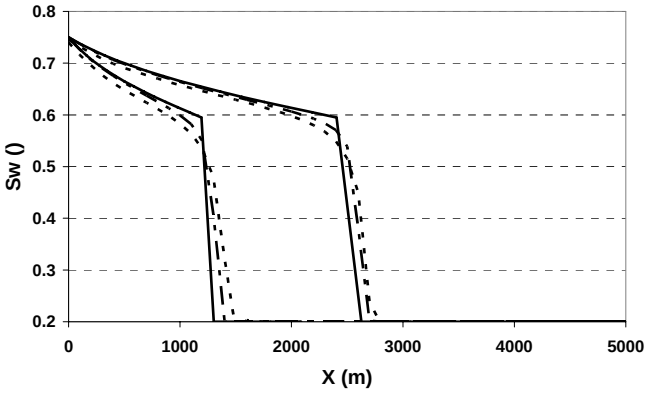

Figure 5. Comparison among water saturation profiles according to the analytical Buckley-Leverett solution (solid line), the streamline solution (dash-dot line), and the implicit simulator solution (small dash line), for two different instants of time.

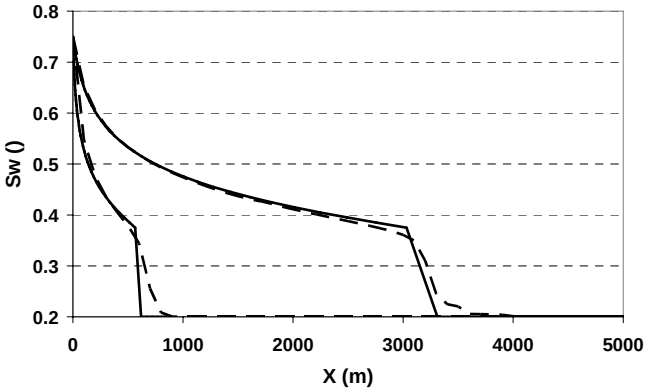

Figure 6. Buckley-Leverett 1D flow with mobility ratio of 10. Analytical (solid line) and numerical streamline solutions (dashed line) are compared for two instants of time.

Figure 7 shows cumulative oil production for the equal mobility case, for both simulators. A good quantitative agreement is obtained.

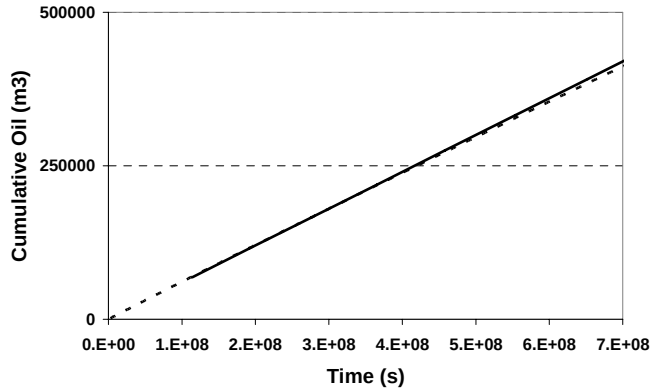

Figure 7. Cumulative oil production comparison for the Buckley-Leverett. Streamline simulator (solid line), and implicit black oil simulator (dashed line).

The second test performed is a quarter of a five-spot tracer flow. The domain is discretized with a 21 x 21 x 1 nodes grid, with 100 m size triangular elements, and a uniform height of 10 m. The rock and fluid properties were the same as for the previous problem. The injection flow rate was 0.01 m^3/s. At the producer, zero pressure was imposed. Saturation profiles along the grid diagonal (from injector to producer) are shown in Figure 8. As there is no closed analytical solution for this problem, the comparison is made only against the full implicit simulator solution. Good quantitative agreement is observed. Again, higher numerical diffusion is detected for the full simulator around the saturation front. The cumulative oil production according to both simulators is compared in Figure 9. Good quantitative agreement is observed.

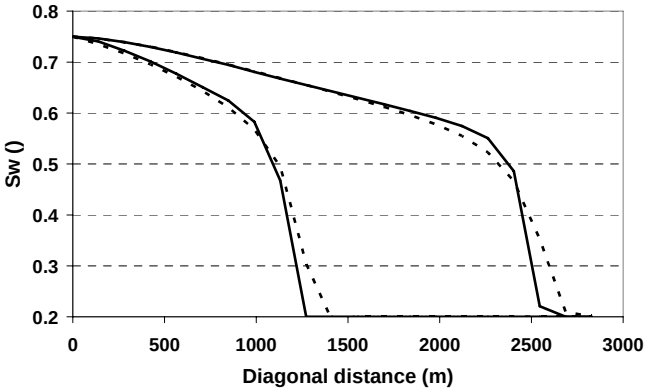

Figure 8. Quarter of a five-spot tracer flow saturation profiles for two different instants of time. Comparison between streamlines simulator (solid line) and fully implicit simulator (dashed line).

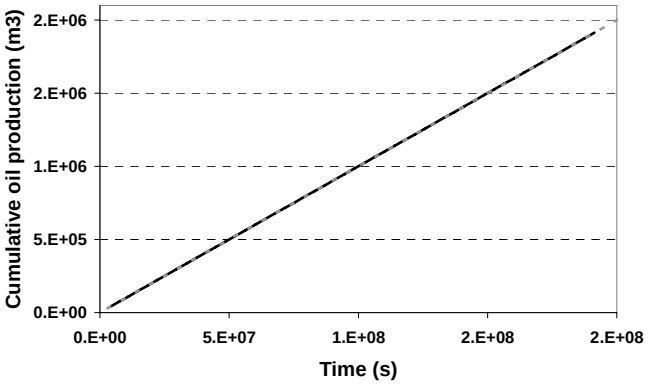

Figure 9. Cumulative oil production from streamlines simulator (solid black line) and full implicit simulator (dashed grey line).

Figures 10 and 11 present the saturation distribution for two instants of time, where the displacement of the saturation front can be observed.

Once again, computer time for the full simulator was 2 to 3 orders of magnitude higher than for the streamlines simulator.

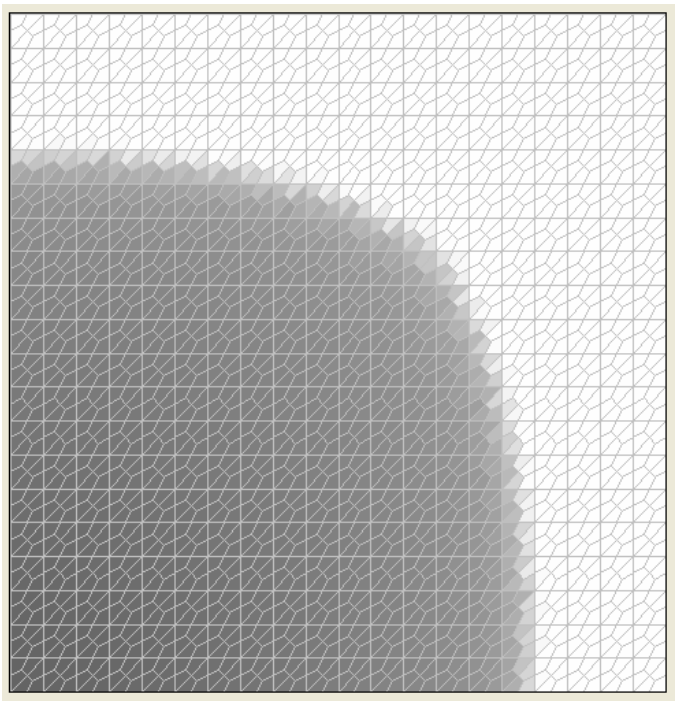

Figure 10. Quarter of a five spot tracer flow horizontal picture. Tracer saturation front is advancing from the lower left corner.

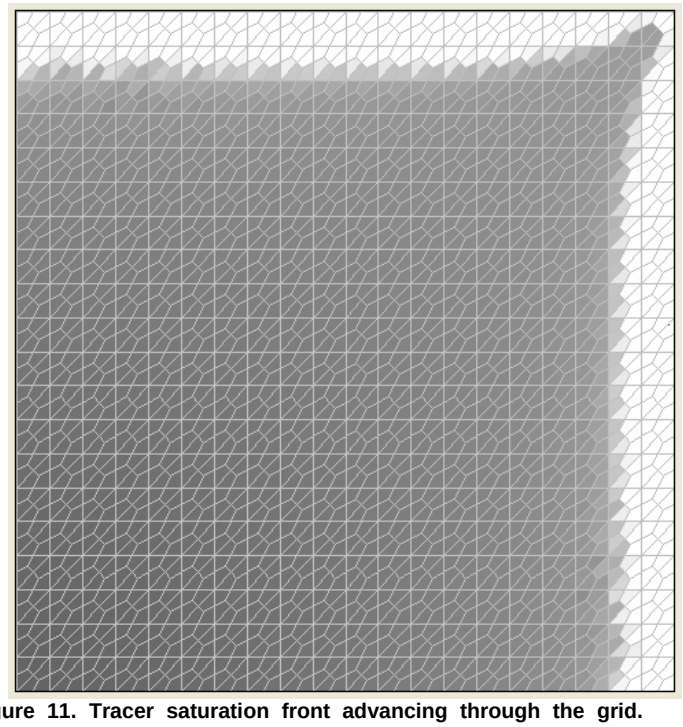

Figure 11. Tracer saturation front advancing through the grid. Tracer flow is represented in gray scale, oil phase fluid is represented in white. Streamlines were removed for the sake of clearness.

Conclusions

A 2D streamline-base simulator for unstructured grids was successfully implemented. The implemented streamline tracing quality criteria allowed the simulator to trace the streamlines field correctly. For the Buckley-Leverett 1D flow problem, the method showed a satisfactory agreement with the analytical solution. The agreement is slightly better than the full implicit simulator used as a reference, due to its lower numerical diffusivity. Results for the quarter of a five spot problem also show good quantitative agreement between both simulators, regarding both the displacement of the saturation front and the cumulative oil production.

The computer performance of the streamlines simulator was much better than for the full simulator, with processing times two to three orders of magnitude lower.

The implemented model, together with the full simulator, constitute a system under development, within a research and development program, to deal with ever increasing levels of complexity in analyzing and predicting oil reservoir behaviors.

References

1. Batycky R.P.: “A three dimensional two-phase field scale streamline simulator”, Phd Thesis, Stanford University, (1997).
2. Menéndez A.N., Pomata M., Valle J., Lacivita A., Kind M.: “Implementación computacional de un simulador de reservorios de petróleo y gas por el método de los volúmenes finitos”, VIII Congreso argentino de mecánica computacional, (2005).
3. Pollock D.W.: “Semianalytical computation of path lines for finite-difference models”, *Ground water*, 1998, 26(6), 743-750.
4. Cordes C., Kinzelbach W.: “Continuous groundwater velocity field and path lines in linear, bilinear, and trilinear finite elements”, *Water resources research*, November 1992, Vol.28, Nº 11, 2903-2911.
5. Prèvost M., Edwards M.G., Blunt M.J.: “Streamline tracing on curvilinear structured and unstructured grids”, *SPE*, 66347.
6. Haegland H.: “Streamline tracing on irregular grids”, Phd Thesis, University of Bergen, Dec. 2003.